

# Single screw extrusion of long discontinuous fiber-reinforced polymers: Pellet motion and heat transfer

Vasudha Kapre<sup>1,2</sup>  | Eduardo Barocio<sup>2,3</sup> | R. Byron Pipes<sup>1,2</sup> 

<sup>1</sup>School of Aeronautics and Astronautics,  
Purdue University, West Lafayette,  
Indiana, USA

<sup>2</sup>Composites Manufacturing and  
Simulation Center, Purdue University,  
West Lafayette, Indiana, USA

<sup>3</sup>School of Mechanical Engineering,  
Purdue University, West Lafayette,  
Indiana, USA

## Correspondence

Vasudha Kapre, School of Aeronautics and Astronautics, Purdue University, West Lafayette, IN 47907, USA.

Email: [vkapre@purdue.edu](mailto:vkapre@purdue.edu)

[Correction added on 22 February 2025,  
after first online publication: The  
affiliation of "Eduardo Barocio" has been  
corrected.]

## Abstract

Single screw extrusion is widely used in material pre-compounding, extrusion additive manufacturing, and injection molding. A single screw extruder has three stages—the solid conveying zone, the transition zone, and the melt-conveying zone. In starve-fed extrusion, the screw channels are partially filled, and melting cannot be analyzed by traditional plug-flow melting models. However, understanding individual pellet motion and melting is an essential precursor to modeling pellet deformation and fiber length attrition in the transition and melt-conveying zones. Therefore, a sequentially coupled framework has been developed to capture individual pellet trajectories and their melting in a single screw extruder. The discrete element method has been used to study motion of long-discontinuous fiber-reinforced pellets which are represented as multi-spheres. Individual pellet melting is captured in a static heat-transfer analysis with dynamic boundary conditions based on the contact information obtained from pellet interactions with its surroundings. Results indicate a translational-conveying motion followed by a rotational-conveying motion of individual pellets as they move along the screw. The rotational-conveying motion coincides with an increase in screw pitch and corresponds to the highest rate of pellet melting. Increasing screw rotation speed reduced the residence time causing insufficient pellet melting. Decreasing the feeding rate did not significantly affect the residence time but resulted in improved melting through increased thermal contacts. Melting is initiated locally on the pellet surface due to thermal contacts and proceeds radially inward. In this process, pellets first experience a molten surface shell before the core reaches melt temperature.

## Highlights

- Multi-sphere representation of LDF reinforced pellets.
- A discrete element model to capture pellet flow in a single screw extruder.
- Individual pellet trajectories extracted from single screw extrusion.

This is an open access article under the terms of the [Creative Commons Attribution-NonCommercial-NoDerivs License](#), which permits use and distribution in any medium, provided the original work is properly cited, the use is non-commercial and no modifications or adaptations are made.

© 2025 The Author(s). *Polymer Composites* published by Wiley Periodicals LLC on behalf of Society of Plastics Engineers.

- A sequentially coupled finite-element model to study LDF pellet heat transfer.
- Study of screw speed and feeding rate on average pellet melting behavior.

**KEY WORDS**

discrete element method, long discontinuous fiber-reinforced pellets, single screw extrusion

## 1 | INTRODUCTION

Long discontinuous fiber (LDF) reinforced pellets are a class of discontinuous composite preform obtained through pultrusion<sup>1</sup> where a fiber tow is impregnated by the matrix polymer and chopped into cylindrical pellets of a uniform length. These pellets are then mixed and melted in a single screw extruder that comprises a helical screw inside a hollow cylindrical barrel that is heated externally. The pellets enter the extruder system at one end in a controlled feeding rate and exit at the other end of the screw as a continuous molten composite with short fibers of various lengths. The orientation state of the extrudate is strongly influenced by the geometry of the extrusion nozzle. In the case of injection molding, the extrudate feeds a die and a mold,<sup>2</sup> while for extrusion deposition additive manufacturing, it feeds a gear pump and nozzle.<sup>3,4</sup> The current work aims to provide a sequentially coupled framework to capture the motion and melting of individual pellets in a single screw extruder. Discrete element method has been used to study the motion of solid cylindrical pellets which are represented as multi-spheres. The single screw extruder and pellet geometries are discussed in the next section, along with the simulation methods. The contact history of a single pellet is isolated and applied as a dynamic boundary condition for a static heat-transfer finite element analysis.

The extruder screw is traditionally divided into three functional zones. The first zone is called the “solid conveying or feed zone” where pellets maintain their initial shape and fiber length. In this zone, the temperature is typically below the glass-transition temperature of the polymer. Rigid-body motion of the individual pellets is primarily driven by gravity and friction.<sup>5,6</sup> For flood-fed extrusion, the pellets are consolidated in the solid-conveying zone. This region is traditionally analyzed by a force-balance of the free-body of a solid plug with surface frictional forces and gravitational body forces.<sup>7–9</sup> Starve-fed extrusion has gained popularity due to its melting efficiency.<sup>10,11</sup> However, analytical models for solid-state granular motion of individual pellets in the partially filled channels of a starve-fed single screw extruder are non-existent.

To study the motion of a granular medium, discrete element method (DEM) is a well-developed approach.<sup>12</sup> This approach uses Newton's laws of motion and Euler's

laws of rotation to capture rigid body motion of individual particles (pellets in the present case). Particle interactions are captured using the principles of contact mechanics.<sup>13–15</sup> DEM has been applied extensively to study pellet flow in a single screw extruder.<sup>16–19</sup> The effect of barrel friction, particle shape and size have been studied to predict the output rate and residence time of granular material.<sup>19–21</sup>

The second zone of a single screw extruder is termed the “transition or compression zone” where the inner diameter of the screw increases gradually, and temperatures rise above the glass transition temperature of the polymer. The pellets in this region soften due to their elevated temperature. They are deformed and dispersed as they transition from discrete solid pellets to a fully molten state as they reach the final “melt-conveying zone.” Maddock and Tadmor<sup>22,23</sup> were among the first to perform experiments and develop theoretical models to capture polymer melting in a single screw extruder. Several other scholars have continued this work.<sup>24–26</sup> However, these studies are all confined to the state of contiguous-solid melting observed in flood-fed extruders.

Numerically, bulk polymer melting has been captured using finite element simulations with two-phase flow.<sup>11,27–29</sup> Recently, Altinkaynak et al.<sup>28</sup> performed experiments to observe melting in starve-fed extrusion of wood-plastic composites. The authors observed dispersed melting in the partially filled regions and the Tadmor-melting mechanism in the fully filled regions. A combination of analytical 2-D models and 3-D finite element simulations were used to predict melting characteristics. Other studies have observed and confirmed dispersed melting for starve-fed extrusion of neat polymers<sup>30</sup> and particulate composites.<sup>31</sup>

Finally, the third zone is called as the “melt-conveying or metering zone” corresponding to the last few channels of the screw with fully molten material. The material exiting the screw has fibers of various lengths, aligned in random orientations. Fiber length attrition is one of the key challenges in the extrusion of LDF pellets as fiber length significantly impacts the thermo-mechanical properties of extruded material.<sup>32,33</sup> Fiber attrition has been observed to occur at various stages throughout the screw.<sup>34–37</sup> However, existing models are mostly based on fluid mechanics and are only applicable to the melt-conveying zone.<sup>38,39</sup> Fiber attrition occurs in two stages, first when fibers are still attached to the pellet, and second when they are in

the polymer melt.<sup>37,40</sup> Since a partially molten pellet has a fully molten shell, the surface fibers are likely to break when subjected to contact interactions with screw, barrel surfaces and neighboring pellets.

Understanding the state of partially molten LDF pellets is an essential precursor to studying fiber attrition mechanisms in the partially molten transition zone of a single screw extruder. Therefore, this study aims to take a discrete approach by tracking individual pellets as they go through the screw and use that information to study individual pellet melting. This information can enable the development of thermo-mechanical models for studying deformation of partially molten LDF pellets and identifying any possible fiber attrition mechanisms.<sup>41</sup> However, this study is limited to pellet motion and heat-transfer. In a sequentially coupled framework, solid pellet motion is first captured using Discrete Element Method (DEM) where feeding rates are in the regime of starve-feeding to reduce computational expense. The contact information obtained from pellet-pellet, pellet-screw and pellet-barrel interactions is used to determine boundary conditions for heat-transfer model of a single pellet. Mechanical deformation and heat generated due to viscous dissipation of polymer are not captured, which result in slower melting of pellets. To observe full melting of individual pellets, the length of the screw has been extended beyond the first two zones to the full length of extruder in DEM and heat-transfer simulations. Although the current work focuses on starve-fed extrusion, it can be applied to flood-fed extrusion following the same approach, at a higher computational expense.

## 2 | THE SINGLE SCREW EXTRUDER IN EXTRUSION DEPOSITION ADDITIVE MANUFACTURING

The geometry of the single screw extruder described in this work is based on the screw of the Composites Additive Manufacturing Research Instrument (CAMRI);

a device developed to perform research on extrusion deposition additive manufacturing at Purdue University.<sup>42</sup> The length-to-diameter (L/D) ratio of the screw is 24:1 with a compression ratio of 3:1. The inner diameter of the barrel is 25.4 mm and the clearance between the flights and barrel is 0.0254 mm. The root diameter increases linearly from 13.97 to 18.80 mm and remains constant for the last five channels. The pitch is constant for the first half of the screw, then increases in the compression zone and decreases again in the last few channels of the melt-conveying zone. The geometry used in this study, shown in Figure 1, was made in SolidWorks.

The purpose of this study is to capture pellet motion and heat transfer in the first two zones of a single screw extruder. To simplify the complex multi-physics nature of the problem in transition zone, heat-transfer has been decoupled from the mechanical deformation of pellets, and viscous dissipation of polymer matrix has not been captured. As heat generated due to polymer viscous dissipation plays a significant role in pellet melting, excluding this mode of heat-transfer resulted in slower melting of pellets, and hence the entire length of the screw was modeled to capture complete pellet melting.

The discrete element method was used to model pellet flow and implemented with the open-source DEM code LIGGGHTS,<sup>43</sup> which is based on the molecular dynamics code LAMMPS,<sup>44</sup> of Sandia National Labs. Pellet contact behavior is captured using a soft particle approach in which penetration distance is used to estimate contact resistance behavior. The modified Hertz model was used to estimate contact force arising from every collision, adopted by.<sup>14</sup> Finally, each LDF pellet was represented by joining 10 spherical geometry particles of 2.5 mm diameter, with a spacing of 1 mm, as shown in Figure 2D. The length of the pellet is 11.5 mm and the diameter is 2.5 mm. DEM simulation parameters are material properties are listed in Table 1. The coefficient of restitution, coefficient of rolling friction and Poisson's ratio were chosen based on commonly accepted properties.<sup>19,45</sup> The Young's Modulus is limited by soft-particle DEM approach and saves computational time. However, the original Young's modulus is used in calculating

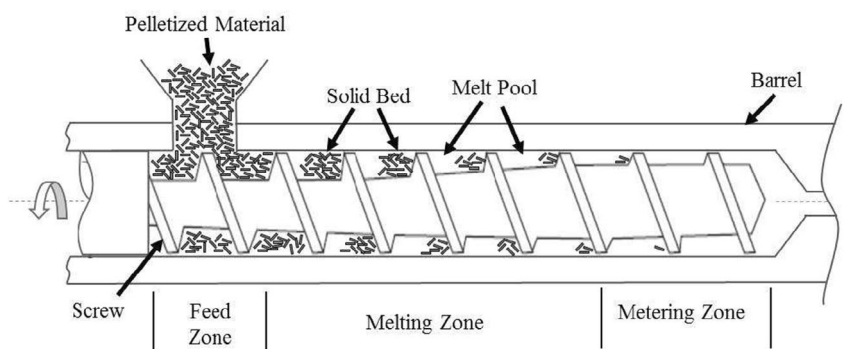
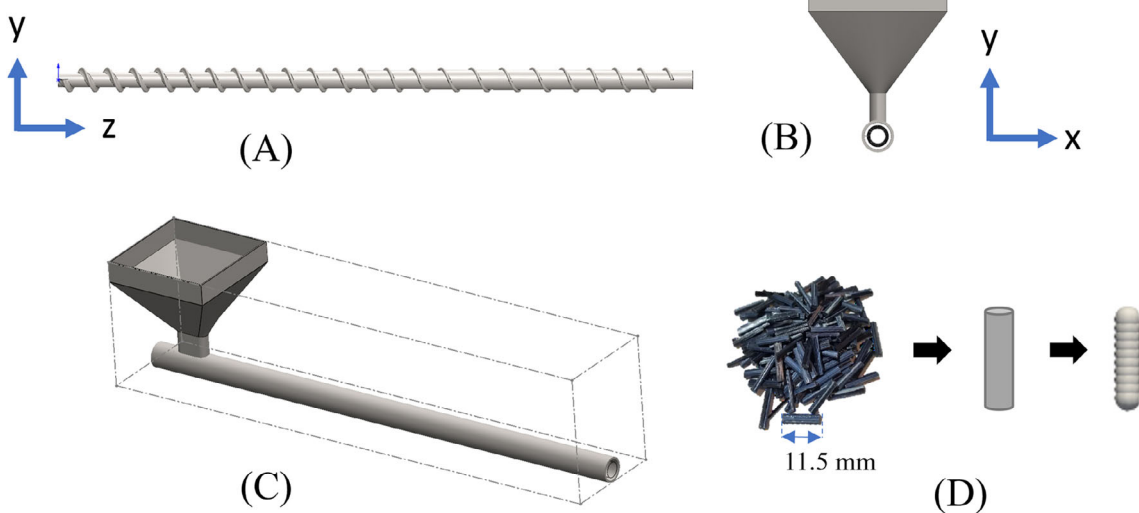


FIGURE 1 Functional zones of a single-screw extruder, borrowed from Reference [42].



**FIGURE 2** Composites Additive Manufacturing Research Instrument single screw extruder assembly. (A) Screw geometry, (B) front view, (C) isometric view of the extruder assembly, and (D) multisphere representation of 40% CF-PPS long discontinuous fiber (LDF) pellets.

**TABLE 1** Discrete element method simulation parameters and material properties.

Parameter	Value
Timestep	1e -6 s
Output request rate	20 Hz
Pellet density	4000 kg/m <sup>3</sup>
Young's Modulus (all)	10 MPa
Original Young's Modulus (screw, barrel)	200 GPa
Original Young's Modulus (pellet)	30 GPa
Poisson's ratio (all)	0.3
Coefficient of restitution (all)	0.3
Coefficient of rolling friction (all)	0.2
Coefficient of friction—pellet-barrel	0.3
Coefficient of friction—pellet-screw	0.2
Coefficient of friction—pellet-pellet	0.3

particle penetration distance during contact interactions. A time step of a millionth of a second was used and outputs were requested at a frequency of 20 Hz. The pellet feeding rates have been kept in the bounds of starve-feeding to reduce computational expense. A detailed parametric investigation of the effect of coefficients of friction has been reported in.<sup>41</sup>

To model heat transfer of a given pellet, FEA software code ABAQUS was used along with the subroutine UMATHT for capturing polymer melting and crystallization kinetics.<sup>46</sup> The material characterization and implementation of UMATHT subroutine was previously developed by<sup>47</sup> and implemented in ADDITIVE3D®, a physics-based

**TABLE 2** Heat-transfer simulation boundary conditions and thermal properties.

Parameter	Value
Screw temperature	600 K
Barrel temperature	600 K
Pellet initial temperature	350 K
Ambient temperature for convection, radiation	600 K
Contact thermal flux coefficient	5000 W/m <sup>2</sup> K
Emissivity	0.85
Ambient convection coefficient	10 W/m <sup>2</sup> K

simulation for extrusion deposition additive manufacturing. Ambient convection, ambient radiation, and thermal contact heat-transfer mechanisms have been captured. The simulation parameters are listed in Table 2.

### 3 | DESCRIPTION OF LDF PELLET MOTION AND HEAT TRANSFER

Pellets are fed into the screw in a controlled manner through a hopper with a small initial velocity of 0.01 m/s. Two materials are defined – one for the metal surfaces that is, screw, barrel and hopper and the second for the pellets. Simulations were carried out with a high-performance computing cluster, provided by Purdue University. Outputs were reported every 0.05 s and post-processed in MATLAB to predict pellet position, velocity, orientation and contact conditions.

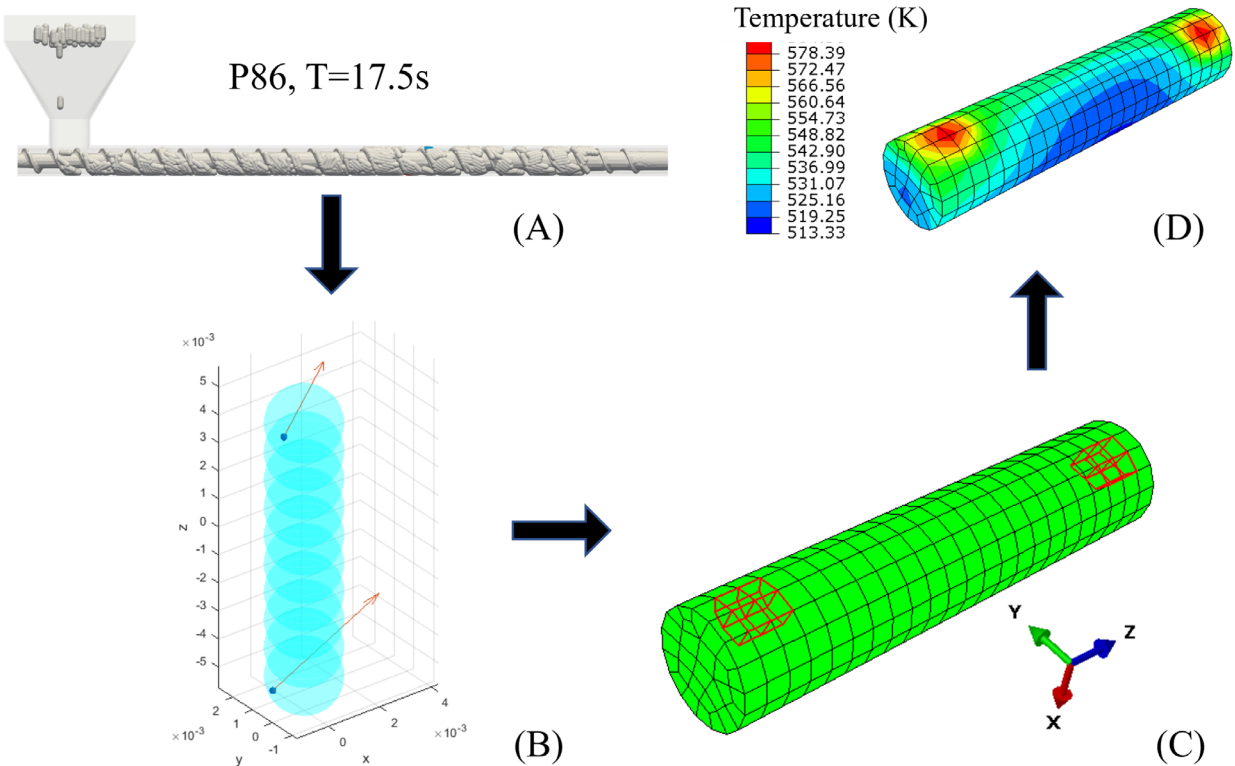


**FIGURE 3** (A) Discrete element method simulation snapshot visualized in Para view. (B) An isolated pellet with two contacts as visualized in MATLAB. (C) Corresponding finite element mesh with contact elements highlighted. (D) Temperature profile showing local hotspots at contacts.

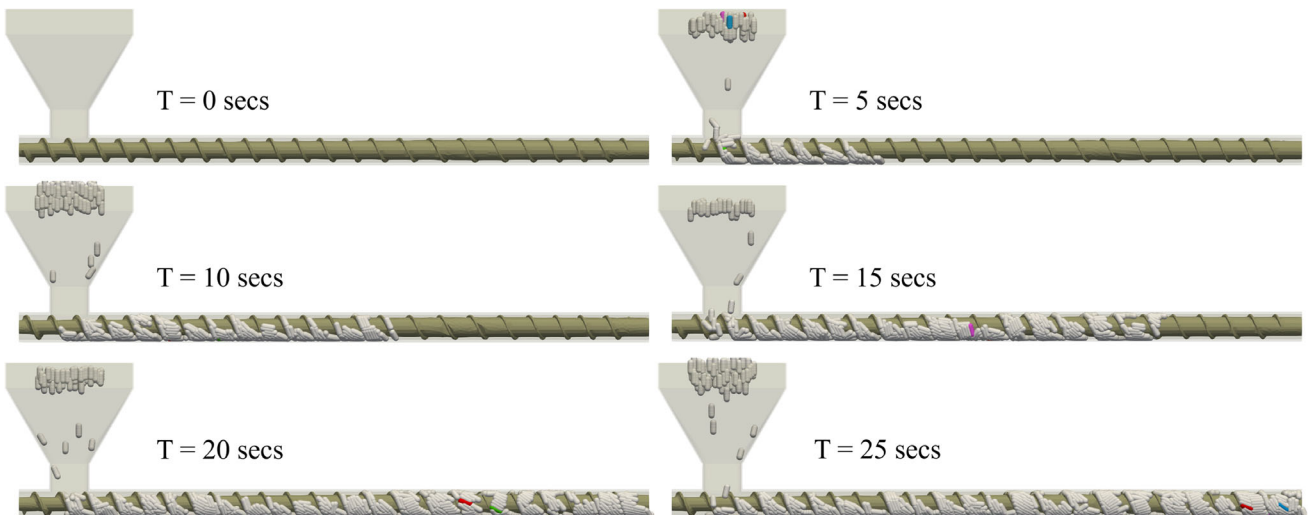


**FIGURE 4** Discrete element simulation visualized in Para view at 5 s increments. Four pellets colored red, blue, pink, and green are tracked for extracting their trajectories.

Once a pellet is chosen, its contact information is used to formulate a static heat transfer problem with dynamic boundary conditions in ABAQUS. The pellet-screw and pellet-barrel contacts are transferred to the pellet FEM mesh where an instantaneous heat flux is applied to replicate the effect of a thermal contact. The

exposed pellet surfaces are subject to ambient convection and radiation where the ambient temperature is same as the screw and barrel temperatures at 600 K. The mapping flowchart is shown in Figure 3. For every pellet at every time-step of the DEM simulation, the contact points of the multisphere geometry are

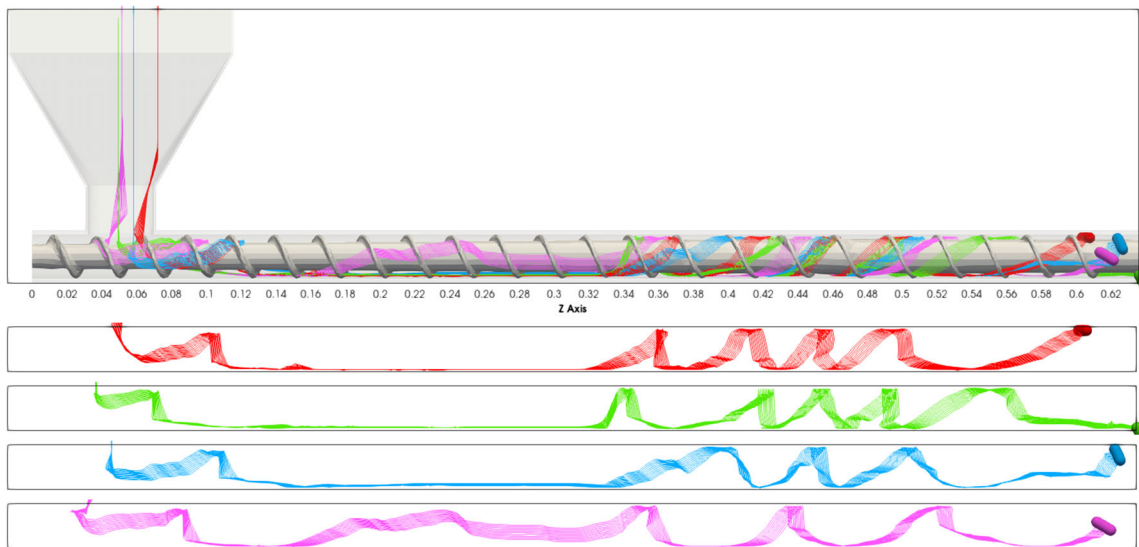


**FIGURE 5** Individual trajectories of four colored pellets isolated and shown as a ribbon tracking the centers of the 10 spheres that form the pellet. Screw length is marked in meters up to 0.62 m.

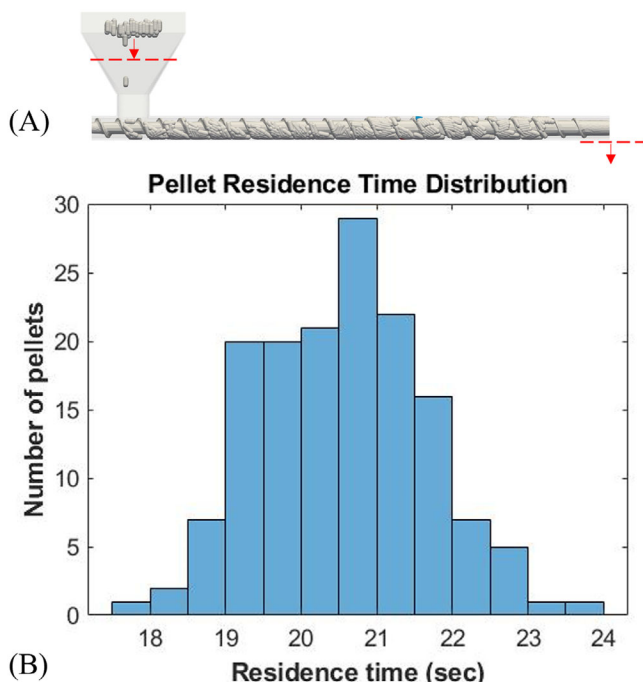


**FIGURE 6** (A) Bounds for residence time calculation. (B) Pellet residence time distribution.

mapped onto a cylindrical FEM mesh of same length and diameter. This process is shown in Figure 3A,B for a pellet with ID 86, at timestep 17.5 s. For the two contact points shown in Figure 3B, the nearest nodes are identified, and the adjacent elements are used to form an element set, as highlighted in red in Figure 3C. This element set is subjected to the thermal contact heat flux at timestep 17.5 s in the heat transfer simulation. The

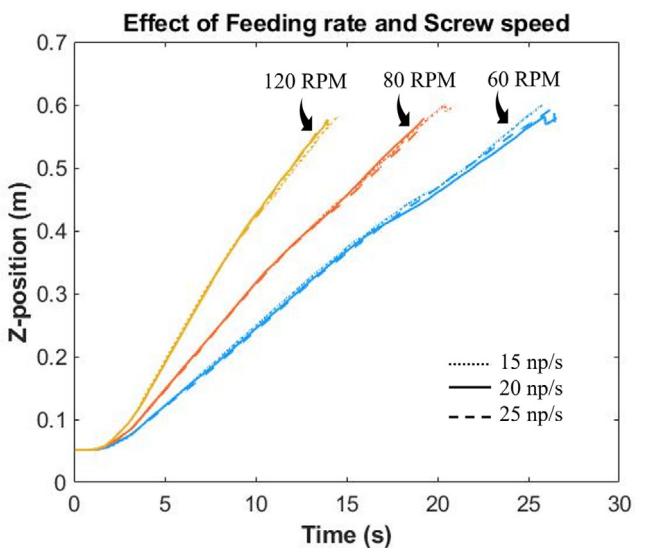


**FIGURE 7** Effect of screw speed and feeding rate on average z-position evolution of pellets.

thermal heat flux is applied as an amplitude curve, and causes local heating as shown in Figure 3D.

Six snapshots of the single screw extruder assembly are taken at 5 s intervals from the start of the simulation. Pellets are inserted in a controlled manner through the hopper at a rate of 25 pellets per second and the screw rotates counterclockwise at 80 revolutions per minute. Four pellets are randomly chosen and colored pink, blue, red, and green for tracking their individual trajectories. Individual pellet trajectories are extracted and shown in Figure 4.

After the initial gravity-driven flow through the hopper, the pellets fall into the second or third channels

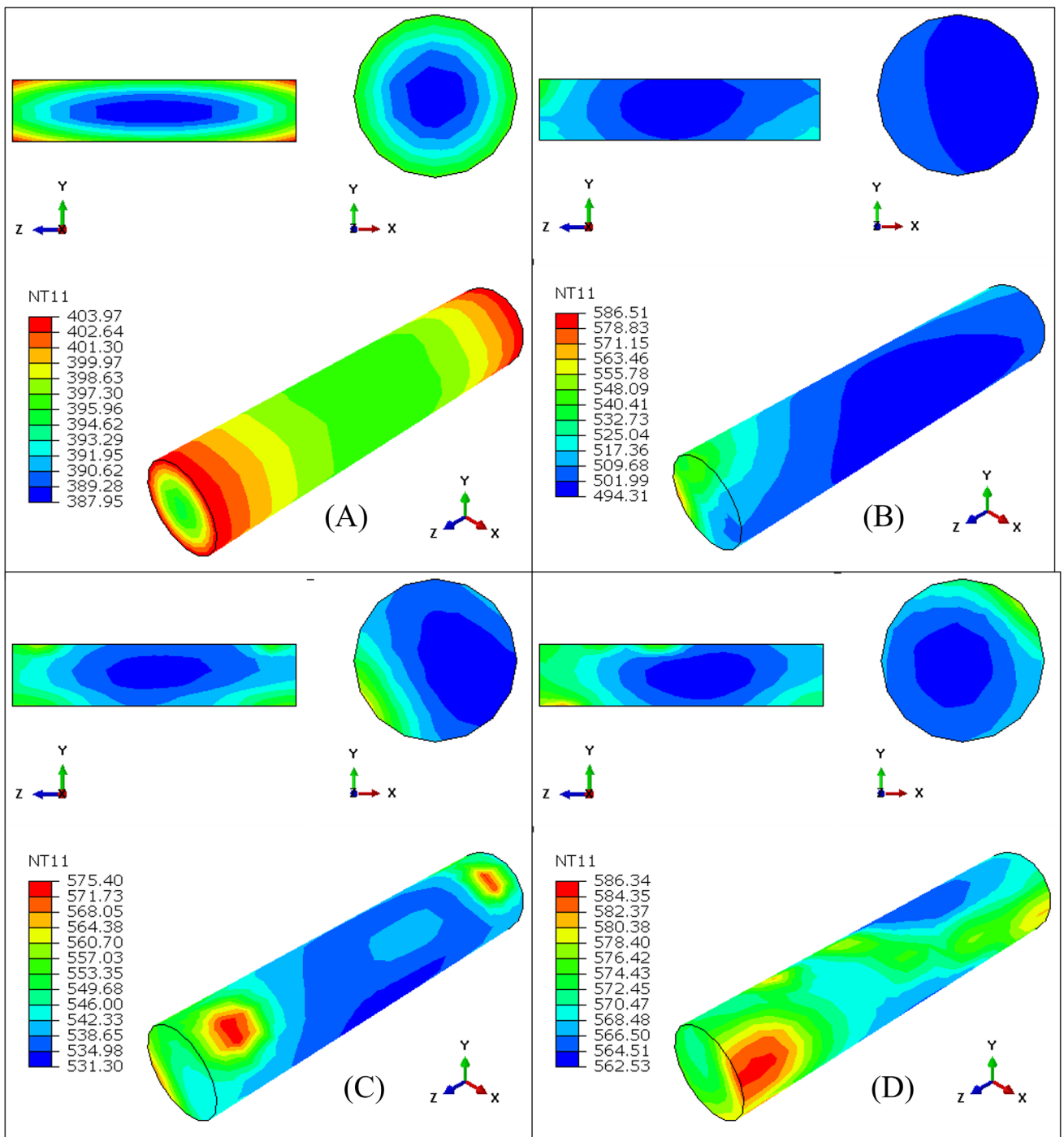


**FIGURE 8** Four instances of pellet degree of melting that varies from 0 for a fully solid material to 1 for a fully molten material. The cut side view, cut front view and isometric view are shown. (A) 5 s, (B) 10 s, (C) 15 s, and (D) 20 s.

of the screw and are pushed forward by the active flight of the screw. Since the screw is starve-fed, the channels remain partially filled as opposed to traditional flood-fed extruder where the channels are fully filled throughout the length of the screw. This allows for relative motion of pellets and reorientation as they mix in a single channel. Within a channel, pellets tend to accumulate near the active flight, aligning with the helix angle of the screw.

Pellets are also driven up and over the screw due to the frictional forces due to pellet-screw and pellet-barrel contacts.

The individual trajectories of four pellets are isolated and extracted, shown in red, blue, pink, and green in Figure 5. Although entering the system at different locations, all four pellets show a similar trajectory where they rest at the bottom of the system while being pushed by

the active flight until 0.3 m of screw length and are then picked up and start rotating along with the screw. This trajectory can be characterized as a translational-conveying followed by rotational-conveying motion. Most pellets (red, green, and blue) seem to rest at the bottom of the extruder assembly for the first half of their journey along the screw, corresponding to the minimum y-coordinate. The region of transition from translational-conveying

motion to rotational-conveying motion coincides with the region of screw where pitch increases; thereby indicating the start of the compression zone.

Residence time is defined as the time spent by a pellet in the extruder system. Specifically, the two red dashed lines, indicated in Figure 6A, were used to determine the residence time of each pellet. The distribution has an average of 20.24 s and lies between 18 and 24 s, as seen

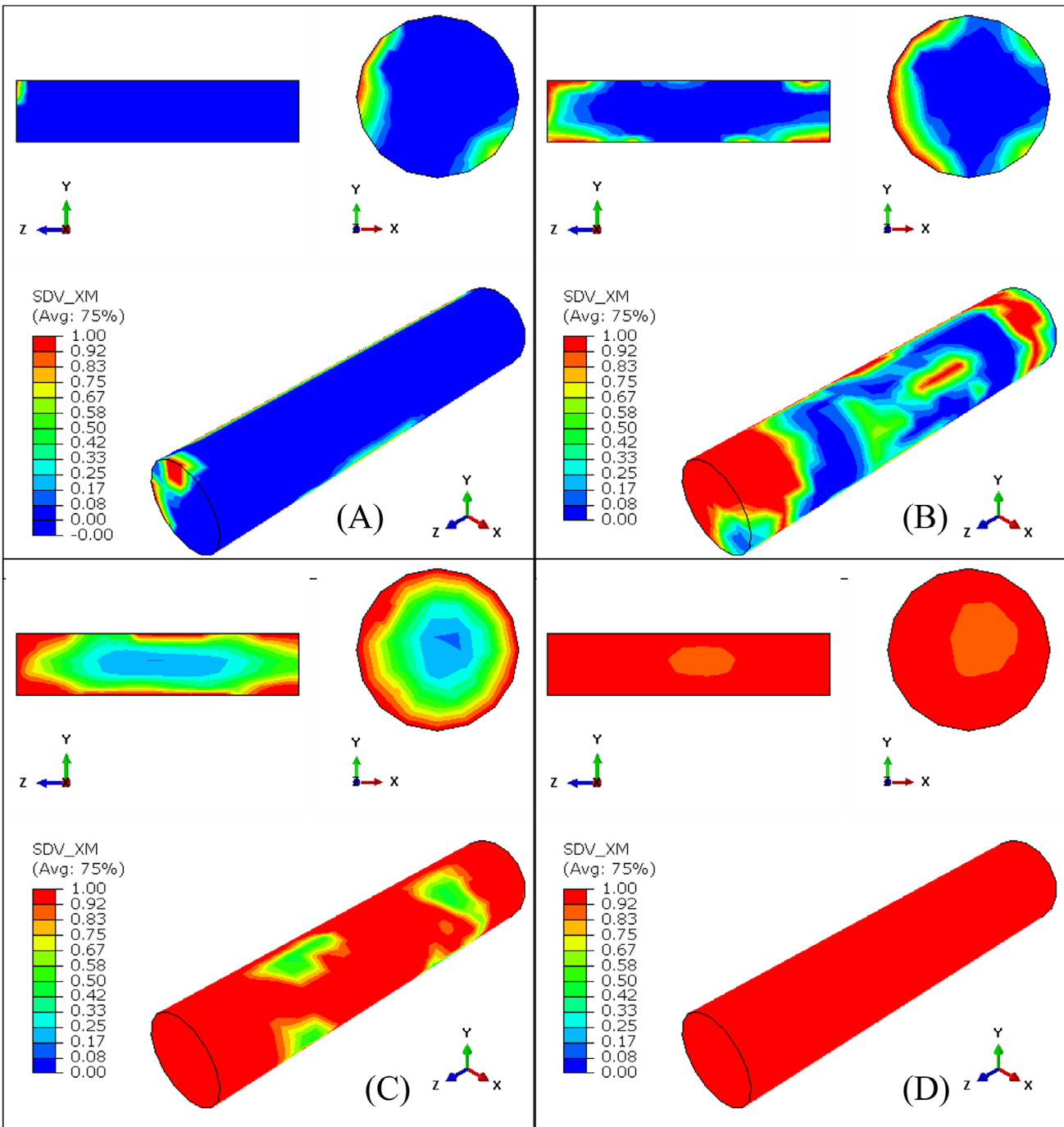


**FIGURE 9** Four instances of pellet degree of melting that varies from 0 for a fully solid material to 1 for a fully molten material. The cut side view, cut front view and isometric view are shown. (A) 5 s, (B) 10 s, (C) 15 s, and (D) 20 s.

in Figure 6B. Residence time has a direct impact on the output flowrate of the bulk and time available for individual pellet melting.

These simulations were repeated for three different screw rotation speeds—60, 80, and 120 RPM and three different feeding rates—15, 20, and 25 pellets per second. The position of center of mass of an average pellet is plotted against time after averaging across all the pellets. This is designated as the ‘z-position’ in Figure 7. Increasing the screw speed from 60 to 120 RPM reduces the average pellet residence time by 50%, as expected. However, changing pellet feeding rate had no measurable effect on pellet residence time.

The four pellets shown in Figure 5 were extracted for heat-transfer and melting simulation. The temperature profile of a single pellet is shown below at four different instances of time. For the first few seconds, pellets undergo free-fall, and heating is purely due to ambient convection and radiation from the environment. This causes the outside edges of the cylinder to be the hottest, as seen in Figure 8A. Once the pellet contacts the hot screw and barrel surfaces, local hotspots form at the points of contact. The thermal contact heating causes local melting as seen in Figure 8C. By the end of the simulation at around 20 s, the pellet is fully heated with the nodal temperatures varying between 562 to 586 K. Additionally, pellet heating is largely radially symmetric as seen in the front and side cut views of Figure 8. The isometric views show the highly dynamic nature of pellet heating, with local hotspots formed during pellet-screw and pellet-barrel contacts.

The pellet degree of melting varies from 0 for the fully solid state to 1 for the fully molten state. Figure 9 shows the evolution of pellet degree of melting at four different instances along with variation of degree of melting across the length and diameter of the pellet. The local hotspots formed due to pellet-screw and pellet-barrel contacts fully melt the polymer locally as seen in of Figure 9B, consistent with the temperature data, pellet melting is radially symmetric with a softer shell and a solid core. By the end of 20 s, the pellet fully melts inside out, as shown in Figure 9D.

Front view of radial pellet melting at time instance 25 s is shown below in Figure 10. The degree of melting extracted from nodes along pellet diameter at mid-span is plotted at various instances of time. At the first instance,  $t = 21$  s, the melting along pellet diameter is not symmetrical. However, as time proceeds, the melting becomes symmetrical, corresponding to the rotational motion of the pellet with all surfaces making contacts with the screw and barrel surfaces.

Combining the pellet position information with the average temperature and average degree of melting, we can identify the region corresponding to the highest rate

of melting. The orange line in Figure 11 indicates pellet position along the length of the screw and the blue line indicates the average degree of melting. The shaded region in Figure 11 corresponds to the maximum degree of melting with a steep change in the slope of the blue curve. The orange curve in the shaded region coincides

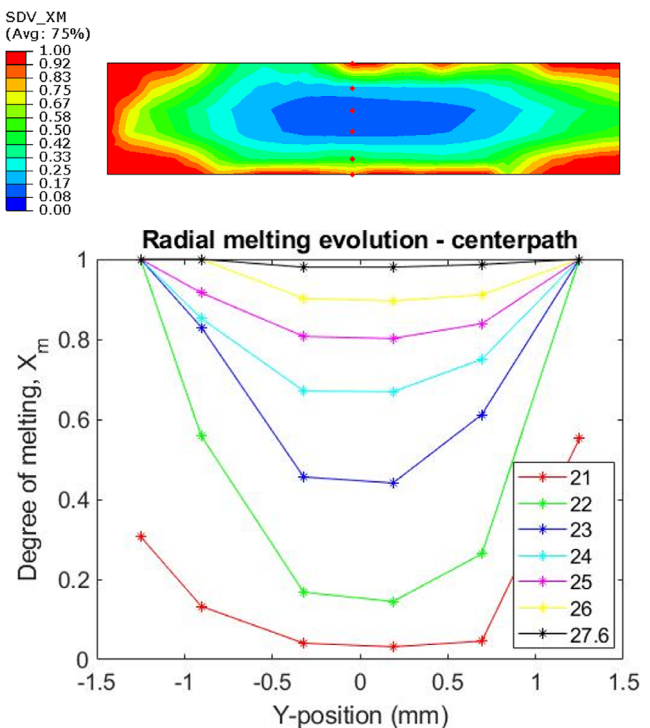


**FIGURE 10** Radial melting profile of a pellet—cut view at 25 s (TOP) and radial melting across mid-span at seven instances (BOTTOM). The legend on plot indicates time in seconds.

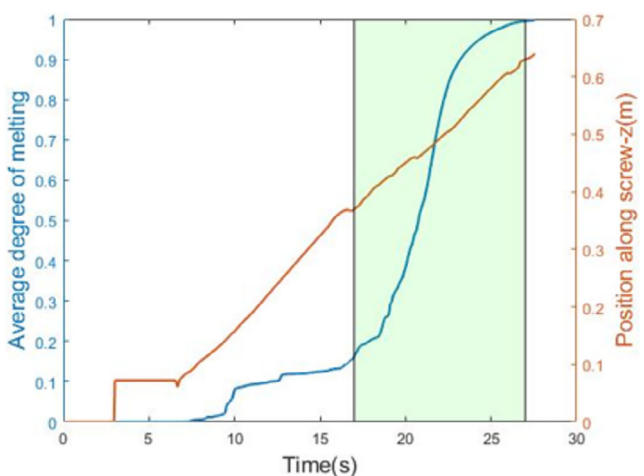
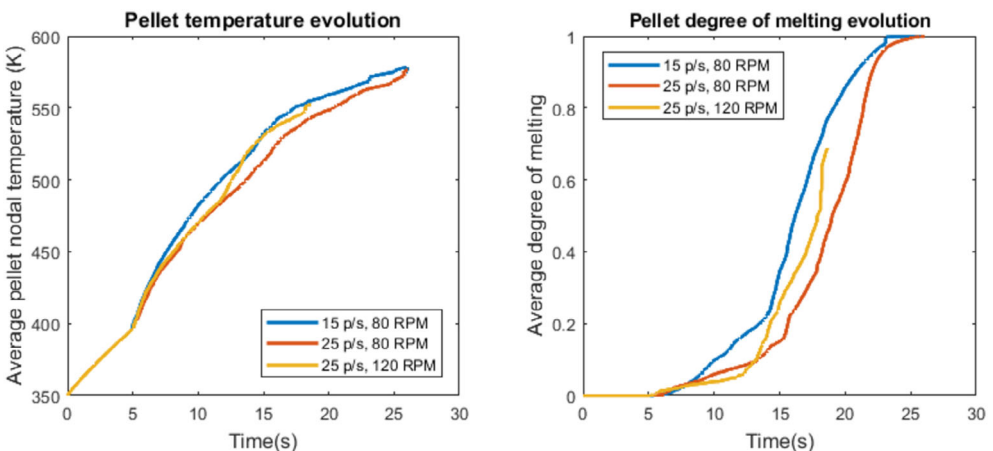


**FIGURE 11** Overlapping pellet distance along the screw with its average temperature and degree of melting. Shaded region corresponds to the rotational = conveying motion with a steep increase in the rate of melting.

**FIGURE 12** Pellet temperature evolution (left) and degree of melting evolution (right) for three different cases varying screw rotation speed and feeding rate.



with the rotational-conveying motion of the pellet, which was identified previously to coincide with the transition and melt-conveying zones of the single screw extruder.

Finally, the effect of screw rotation speed and pellet feeding rate on average melting behavior of individual pellets was studied. Three different DEM simulations were performed: 15 p/s, 80 RPM (blue); 25 p/s, 80 RPM (red) and 25 p/s, 120 RPM (yellow). From each simulation, four randomly chosen pellets were used for the heat-transfer analysis, and their average is shown in Figure 12. Increasing feeding rate from 15 to 25 pellets per second, we observed that red curve is below the blue curve indicating that fuller channels result in lower temperatures and lower degree of melting. On the other hand, increasing screw speed increases the rate of pellet melting, as indicated by the yellow and red curves in Figure 12 (right). In addition, a screw speed of 120 RPM (yellow curve) does not allow the pellets to fully melt before they exit the screw.

## 4 | CONCLUSIONS

This paper has studied the motion and heat-transfer of long-discontinuous fiber reinforced polymer pellets through a single screw extruder. Pellet flow was captured using discrete element method, and the cylindrical pellets were represented as multi-spheres. Individual pellet trajectories were extracted to characterize the motion of a single pellet in starve-fed extrusion. A sequentially coupled framework was developed to model the heat-transfer and melting of an individual pellet. The dynamic heat-transfer boundary conditions were obtained from the contact information of DEM model. The main findings of the study are as follows:

Screw channels were partially filled with pellets piled near the active flight of the screw. Pellets stayed at the

bottom of the barrel hugging the active flight for roughly the first half of the screw length as they were pushed forward by the active flight. Then they started rotating along with the screw and continued until they exited the extruder system. The transition from translational to rotational motion occurs due to the increase in the diameter of the screw-root and reduction in pitch, defined as a characteristic of the compression zone of a single-screw extruder. The average residence time increased by 50% when the screw rotation speed was doubled from 50 to 80 RPM at a constant feeding rate of 20 pellets per second. Changing the feeding rate from 15 to 25 pellets per second did not have a significant effect on the average pellet residence time.

Individual pellet heat-transfer results indicated a radially symmetric outside-in heating. Thermal contacts due to pellet-screw and pellet-barrel interaction caused hotspots, locally melting the polymer. Combining the pellet motion information with its average degree of melting, the highest rate of melting was found to occur during the rotational-conveying motion of the pellet in the second half of the screw. Increasing the screw rotation speed led to insufficient melting, as the residence time was decreased allowing shorter durations for the pellet to melt. Decreasing the feeding rate caused more efficient melting due to increased pellet-screw and pellet-barrel contacts. This agrees with other studies that have observed starving the extruder system to cause efficient melting.

Based on these observations, it can be concluded that screw geometry has a significant effect of pellet motion. Further development of these models with a focus on individual pellet deformation can help in understanding fiber length attrition in the compression zone of a starved single screw extruder.

## DATA AVAILABILITY STATEMENT

The data that support the findings of this study are available from the corresponding author upon reasonable request.

**ORCID**

Vasudha Kapre  <https://orcid.org/0000-0001-8057-0211>  
R. Byron Pipes  <https://orcid.org/0000-0002-3644-9489>

**REFERENCES**

1. Ishikawa T, Amaoka K, Masubuchi Y, et al. Overview of automotive structural composites technology developments in Japan. *Compos Sci Technol.* 2018;155:221-246. doi:[10.1016/j.compscitech.2017.09.015](https://doi.org/10.1016/j.compscitech.2017.09.015)
2. Inoue A, Morita K, Tanaka T, Arao Y, Sawada Y. Effect of screw design on fiber breakage and dispersion in injection-molded long glass-fiber-reinforced polypropylene. *J Compos Mater.* 2015;49(1):75-84. doi:[10.1177/0021998313514872](https://doi.org/10.1177/0021998313514872)
3. Barocio E, Brenken B, Favaloro A, Bogdanor M, Pipes RB. Extrusion deposition additive manufacturing with fiber-reinforced thermoplastic polymers. *Structure and Properties of Additive Manufactured Polymer Components.* Woodhead Publishing; 2020:191-219. doi:[10.1016/B978-0-12-819535-2.00007-7](https://doi.org/10.1016/B978-0-12-819535-2.00007-7)
4. Pricci A, de Tullio MD, Percoco G. Analytical and numerical models of thermoplastics: a review aimed to pellet extrusion-based additive manufacturing. *Polymers.* 2021;13(18):3160. doi:[10.3390/polym13183160](https://doi.org/10.3390/polym13183160)
5. Chung CI. *Extrusion of Polymers: Theory & Practice.* Carl Hanser Verlag GmbH & Co. KG; 2019. doi:[10.1016/C2018-0-05367-0](https://doi.org/10.1016/C2018-0-05367-0)
6. Rauwendaal C. *Polymer Extrusion.* Carl Hanser Verlag GmbH & Co. KG; 2014. doi:[10.3139/9781569905395](https://doi.org/10.3139/9781569905395)
7. Broyer E, Tadmor Z. Solids conveying in screw extruders, part I: a modified isothermal model. *Polym Eng Sci.* 1972;12(1):12-24. doi:[10.1002/PEN.760120103](https://doi.org/10.1002/PEN.760120103)
8. Derezhinski SJ. Control volume analysis of feed flow in extruders. *J Reinf Plast Compos.* 1999;18(5):437-453. doi:[10.1177/073168449901800504](https://doi.org/10.1177/073168449901800504)
9. Waku A, Oi T, Sakurai S. Solid Conveying in Extruders. *Society of Plastics Engineers.* 1956;1997(574):20-29. doi:[10.2208/JSCET.1997.574\\_97](https://doi.org/10.2208/JSCET.1997.574_97)
10. Elemans PHM, Van Wunnik JM. The effect of feeding mode on dispersive mixing efficiency in single-screw extrusion. *Polym Eng Sci.* 2001;41(7):1099-1106. doi:[10.1002/PEN.10810](https://doi.org/10.1002/PEN.10810)
11. Wilczyński K, Nastaj A, Wilczyński KJ. Melting model for starve fed single screw extrusion of thermoplastics. *Int Polym Process.* 2013;28(1):34-42. doi:[10.3139/217.2640](https://doi.org/10.3139/217.2640)
12. Cundall PA, Strack ODL. A discrete numerical model for granular assemblies. *Géotechnique.* 1979;29(1):47-65. doi:[10.1680/geot.1979.29.1.47](https://doi.org/10.1680/geot.1979.29.1.47)
13. Di Renzo A, Di Maio FP. Comparison of contact-force models for the simulation of collisions in DEM-based granular flow codes. *Chem Eng Sci.* 2004;59(3):525-541. doi:[10.1016/j.ces.2003.09.037](https://doi.org/10.1016/j.ces.2003.09.037)
14. Di Renzo A, Di Maio FP. An improved integral non-linear model for the contact of particles in distinct element simulations. *Chem Eng Sci.* 2005;60(5):1303-1312. doi:[10.1016/j.ces.2004.10.004](https://doi.org/10.1016/j.ces.2004.10.004)
15. Rojek J. *Contact Modeling in the Discrete Element Method. Courses Lectures.* Vol 585. CISM International Centre for Mechanical Sciences; 2018:177-228. doi:[10.1007/978-3-319-90155-8\\_4](https://doi.org/10.1007/978-3-319-90155-8_4)
16. Guo Y, Curtis JS. Discrete element method simulations for complex granular flows. *Annu Rev Fluid Mech.* 2015;47(1):21-46. doi:[10.1146/annurev-fluid-010814-014644](https://doi.org/10.1146/annurev-fluid-010814-014644)
17. Hyvärinen M, Jabeen R, Kärki T. The modelling of extrusion processes for polymers-a review. *Polymers.* 2020;12(6):1306. doi:[10.3390/polym12061306](https://doi.org/10.3390/polym12061306)
18. Michelangeli OP, Yamanoi M, Gaspar-Cunha A, Covas JA. Modelling pellet flow in single extrusion with DEM. *Proc Inst Mech Eng Part E: J Process Mech Eng.* 2011;225(4):255-268. doi:[10.1177/0954408911418159](https://doi.org/10.1177/0954408911418159)
19. Moysey PA, Thompson MR. Modelling the solids inflow and solids conveying of single-screw extruders using the discrete element method. *Powder Technol.* 2005;153(2):95-107. doi:[10.1016/j.powtec.2005.03.001](https://doi.org/10.1016/j.powtec.2005.03.001)
20. Liu K, Zitzenbacher G, Laengauer M, Kneidinger C. Influence of Pellet Shape on the External Coefficient of Friction of Polypropylene and on the Mass Flow Rate of a Single Screw Extruder. *AIP Conference Proceedings.* Vol 1593. American Institute of Physics; 2014:101-105. doi:[10.1063/1.4873743](https://doi.org/10.1063/1.4873743)
21. Michelangeli OP, Gaspar-Cunha A, Covas JA. The influence of pellet-barrel friction on the granular transport in a single screw extruder. *Powder Technol.* 2014;264:401-408. doi:[10.1016/j.powtec.2014.05.066](https://doi.org/10.1016/j.powtec.2014.05.066)
22. Maddock BH. A visual analysis of flow and mixing in extruder screws. *SPE J.* 1959;15:383-389.
23. Tadmor Z. Fundamentals of plasticating extrusion. I. A theoretical model for melting. *Polym Eng Sci.* 1966;6(3):185-190. doi:[10.1002/pen.760060303](https://doi.org/10.1002/pen.760060303)
24. Lindt JT. Mathematical modeling of melting of polymers in a single-screw extruder a critical review. *Polym Eng Sci.* 1985;25(10):585-588. doi:[10.1002/pen.760251002](https://doi.org/10.1002/pen.760251002)
25. Mount EM, Watson JG, Chung CI. Analytical melting model for extrusion: melting rate of fully compacted solid polymers. *Polym Eng Sci.* 1982;22(12):729-737. doi:[10.1002/pen.760221202](https://doi.org/10.1002/pen.760221202)
26. Rauwendaal C. Melting theory for temperature-dependent fluids, exact analytical solution for power-law fluids. *Adv Polym Technol.* 1991;11(1):19-25. doi:[10.1002/adv.1991.060110104](https://doi.org/10.1002/adv.1991.060110104)
27. Wilczyński KJ, Buziak K. A computer model of starve fed single screw extrusion of wood plastic composites. *Polymers.* 2021;13(8):1-17. doi:[10.3390/polym13081252](https://doi.org/10.3390/polym13081252)
28. Altinkaynak A, Gupta M, Spalding MA, Crabtree SL. Melting in a single screw extruder: experiments and 3D finite element simulations. *Int Polym Process.* 2011;26(2):182-196. doi:[10.3139/217.2419](https://doi.org/10.3139/217.2419)
29. Lewandowski A, Wilczyński K. Global modeling of single screw extrusion with slip effects. *Int Polym Process.* 2019;34(1):81-90. doi:[10.3139/217.3653](https://doi.org/10.3139/217.3653)
30. Isherwood DP, Pieris RN, Kassatly J. The effect of metered starve feeding on the performance of a small extruder. *J Eng Ind.* 1984;106:132-136.
31. Thompson MR, Donoian G, Christiano JP. Melting mechanism of a starved-fed single-screw extruder for calcium carbonate filled polyethylene. *Polym Eng Sci.* 2000;40(9):2014-2026. doi:[10.1002/pen.11334](https://doi.org/10.1002/pen.11334)
32. Pipes RB, Hearle JWS, Beaussart AJ, Okine RK. Influence of fiber length on the viscous flow of an oriented fiber assembly. *J Compos Mater.* 1991;25(10):1379-1390. doi:[10.1177/002199839102501008](https://doi.org/10.1177/002199839102501008)
33. Capela C, Oliveira SE, Pestana J, Ferreira JAM. Effect of fiber length on the mechanical properties of high dosage carbon reinforced. *Proc Struct Integr.* 2017;5:539-546. doi:[10.1016/J.PROSTR.2017.07.159](https://doi.org/10.1016/J.PROSTR.2017.07.159)
34. Gupta VB, Mittal RK, Sharma PK, Mennig G, Wolters J. Some studies on glass fiber-reinforced polypropylene. Part I: Reduction in fiber length during processing. *Polym Compos.* 1989;10(1):8-15. doi:[10.1002/pc.750100103](https://doi.org/10.1002/pc.750100103)

35. Lafranche E, Krawczak P, Ciolkzyk J, Maugey J. Injection moulding of long glass fiber reinforced polyamide 66: processing conditions/microstructure/flexural properties relationship. *Adv Polym Technol.* 2005;24(2):114-131. doi:[10.1002/adv.20035](https://doi.org/10.1002/adv.20035)
36. von Turkovich R, Erwin L. Fiber fracture in reinforced thermoplastic processing. *Polym Eng Sci.* 1983;23(13):743-749. doi:[10.1002/pen.760231309](https://doi.org/10.1002/pen.760231309)
37. Wolf HJ. Screw plasticating of discontinuous fiber filled thermoplastic: mechanisms and prevention of fiber attrition. *Polym Compos.* 1994;15(5):375-383. doi:[10.1002/pc.750150508](https://doi.org/10.1002/pc.750150508)
38. Phelps JH, Abd El-Rahman AI, Kunc V, Tucker CL. A model for fiber length attrition in injection-molded long-fiber composites. *Compos Part A: Appl Sci Manuf.* 2013;51:11-21. doi:[10.1016/j.compositesa.2013.04.002](https://doi.org/10.1016/j.compositesa.2013.04.002)
39. Durin A, De Micheli P, Ville J, Inceoglu F, Valette R, Vergnes B. A matricial approach of fibre breakage in twin-screw extrusion of glass fibres reinforced thermoplastics. *Compos Part A: Appl Sci Manuf.* 2013;48(1):47-56. doi:[10.1016/j.compositesa.2012.12.011](https://doi.org/10.1016/j.compositesa.2012.12.011)
40. Bechara A, Goris S, Yanev A, Brands D, Osswald T. Novel modeling approach for fiber breakage during molding of long fiber-reinforced thermoplastics. *Phys Fluids.* 2021;33(7). doi:[10.1063/5.0058693](https://doi.org/10.1063/5.0058693)
41. Kapre V. Fiber length attrition of long-discontinuous fiber reinforced polymer pellets in a single screw extruder. 2024. doi:[10.25394/PGS.27961422.v1](https://doi.org/10.25394/PGS.27961422.v1)
42. Barocio E. *Fusion Bonding of Fiber Reinforced Semi-Crystalline Polymers in Extrusion Deposition Additive Manufacturing*. Purdue University; 2020. doi:[10.25394/PGS.7434068.v1](https://doi.org/10.25394/PGS.7434068.v1)
43. Kloss C, Goniva C. LIGGGHTS—open source discrete element simulations of granular materials based on Lammps. *Supplemental Proceedings.* Wiley; 2011:781-788. doi:[10.1002/978111802142.ch94](https://doi.org/10.1002/978111802142.ch94)
44. Thompson AP, Aktulga HM, Berger R, et al. LAMMPS—a flexible simulation tool for particle-based materials modeling at the atomic, meso, and continuum scales. *Comput Phys Commun.* 2022;271:108171. doi:[10.1016/j.cpc.2021.108171](https://doi.org/10.1016/j.cpc.2021.108171)
45. Campbell GA, Dontula N. Solids transport in extruders. *Int Polym Process.* 1995;10(1):30-35. doi:[10.3139/217.950030](https://doi.org/10.3139/217.950030)
46. Velisaris CN, Seferis JC. Crystallization kinetics of polyetheretherketone (peek) matrices. *Polym Eng Sci.* 1986;26(22):1574-1581. doi:[10.1002/pen.760262208](https://doi.org/10.1002/pen.760262208)
47. Brenken B, Barocio E, Favaloro A, Kunc V, Pipes RB. Development and validation of extrusion deposition additive manufacturing process simulations. *Addit Manuf.* 2019;25:218-226. doi:[10.1016/J.ADDMA.2018.10.041](https://doi.org/10.1016/J.ADDMA.2018.10.041)

**How to cite this article:** Kapre V, Barocio E, Pipes RB. Single screw extrusion of long discontinuous fiber-reinforced polymers: Pellet motion and heat transfer. *Polym Compos.* 2025; 46(11):10102-10113. doi:[10.1002/pc.29606](https://doi.org/10.1002/pc.29606)